

# Neutrino counting experiments and non-unitarity from LEP and future experiments

F. J. Escrihuela <sup>1,\*</sup> L. J. Flores <sup>2,†</sup> and O. G. Miranda <sup>2‡</sup>

<sup>1</sup> *AHEP Group, Institut de Física Corpuscular –  
C.S.I.C./Universitat de València, Parc Científic de Paterna.*

*C/Catedrático José Beltrán, 2 E-46980 Paterna (València) - SPAIN and*

<sup>2</sup> *Departamento de Física, Centro de Investigación y de Estudios Avanzados del IPN  
Apdo. Postal 14-740 07000 Mexico, DF, Mexico*

## Abstract

Non-unitarity of the neutrino mixing matrix is expected in many scenarios with physics beyond the Standard Model. Motivated by the search for deviations from unitary, we study two neutrino counting observables: the neutrino-antineutrino gamma process and the invisible  $Z$  boson decay into neutrinos. We report on new constraints for non-unitarity coming from the first of this observables. We study the potential constraints that future collider experiments will give from the invisible decay of the  $Z$  boson, that will be measured with improved precision.

---

\*Electronic address: franesfe@alumni.uv.es

†Electronic address: jflores@fis.cinvestav.mx

‡Electronic address: omr@fis.cinvestav.mx

## I. INTRODUCTION

Particle physics is currently in an era of great progress, with new experiments [1–5] envisaged for the future. The existence of neutrino oscillations, as well as the discovery of the Higgs Boson are the main motivations for the development of new experiments that will measure the standard physics parameters with unprecedented precision, while also searching for new physics.

In the Standard Model picture, there are three active light neutrinos with an interaction governed by the  $SU(2)_L \otimes U(1)_Y$  electroweak symmetry [6]. The neutrino mixing in this case is described by a unitary  $3 \times 3$  matrix. If more (heavy) neutrino states exist, the corresponding mixing will be bigger and the matrix will have, at some level, a deviation from unitarity. Such a picture has been studied since long time ago [7–9] and, more recently, a description in terms of a triangular parametrization has been discussed [10–13].

In the presence of such a non-unitary (NU) mixing, neutrino counting experiments at high energies will differ from the Standard Model prediction [14]. This is the case of the invisible decay width of the  $Z$  boson [15, 16] and also of the  $\nu\bar{\nu}\gamma$  measurements [17]. As far as we know, no constraints on non-unitarity have been reported from the  $\nu\bar{\nu}\gamma$  process. On the opposite side, current measurement of the invisible decay of the  $Z$  boson lies two standard deviations below the Standard Model prediction, a measurement that has already been studied with detail [18]. On the other hand, different proposals for the future generation of collider experiments are currently under development [19], such as ILC [1, 20, 21], FCC-ee [2, 22], and CEPC [3, 4, 23, 24]. These proposals will be running at the very high energy regime, searching for new physics and measuring the Standard Model parameters in a different energy scale. They will also test physics at relatively lower energies, in order to improve the measurements on already known observables. In particular, it is expected that the invisible  $Z$  decay width will be measured with improved precision, if compared to the current reported measurement by LEP [15, 16].

In this work we study the constraints arising from the neutrino counting experiments around the  $Z$  peak, specifically using data from  $\nu\bar{\nu}\gamma$  measurement. We also analyze the invisible  $Z$  decay to have a complete scenario in the same framework and study the potential of future neutrino counting experiments in the same energy regime to constraint the non-unitary parameters, and compare these perspectives with the current constraints. We will

show that the perspectives in these future experiments are very promising.

In section II, we will start the discussion by describing the non-unitarity formalism that we will use. Then, in section III we present the analysis used to obtain constraints on the nonunitary parameters, as well as the found results and perspectives for future experiments. Finally, in section IV we present our conclusions.

## II. NON-UNITARITY, INVISIBLE $Z$ DECAY AND $\nu\bar{\nu}\gamma$

Non-unitarity has been subject to study for a long time [6, 7, 25, 26]. Recent constraints can be found elsewhere [11, 27], either considering only the restrictions coming from neutrino experiments, or including the ones from charged leptons. In both cases it is useful to consider the mixing matrix as describing the transformation of three light neutrinos and  $n - 3$  neutral heavy leptons. In this way, one can see the  $U^{n \times n}$  matrix as the combination of four submatrices [28]

$$U^{n \times n} = \begin{pmatrix} N & S \\ V & T \end{pmatrix}, \quad (1)$$

with  $N$  a  $3 \times 3$  submatrix in the light neutrino sector, and  $S$  the  $3 \times (n - 3)$  submatrix that describes the mixing of the extra heavy isosinglet states.

One useful way to parametrize the non-unitarity of the mixing matrix  $N$  is the triangular parametrization [10]

$$N = N^{NP}U = \begin{pmatrix} \alpha_{11} & 0 & 0 \\ \alpha_{21} & \alpha_{22} & 0 \\ \alpha_{31} & \alpha_{32} & \alpha_{33} \end{pmatrix} U, \quad (2)$$

where  $U$  is the unitary PMNS mixing matrix for the standard  $3 \times 3$  case and  $N^{NP}$  parametrizes the deviations from unitarity. In this way, we can encode all the parameters of the general description [6, 29], for an arbitrary number of additional neutrino states, in a compact notation. In this general framework, we can describe the non-unitary phenomenology by using the three real parameters  $\alpha_{11}$ ,  $\alpha_{22}$ , and  $\alpha_{33}$  (all of them close to one) plus other three complex parameters  $\alpha_{21}$ ,  $\alpha_{31}$ ,  $\alpha_{32}$  that contains extra CP violating phases and whose magnitude is small.

In what follows we will discuss two neutrino counting observables in the context of this

triangular parametrization.

### A. The invisible $Z$ decay

In the standard unitary limit, the branching for the invisible  $Z$  decay into neutrinos will be given by [30, 31],

$$\Gamma_{inv} = N_\nu \Gamma_{\nu\bar{\nu}} \quad (3)$$

with  $N_\nu$  the effective number of neutrino families and [31]

$$\Gamma_{\nu\bar{\nu}} = \frac{G_F M_Z^3}{12\sqrt{2}\pi}. \quad (4)$$

Experimentally, the ratio  $\Gamma_{inv}/\Gamma_{\ell\bar{\ell}}$  has been measured with greater experimental precision than  $\Gamma_{inv}$  alone [15, 31]. Therefore, the number of light active neutrinos can be estimated from this relation, that in the Standard Model is given by [15]

$$R_{inv}^0 \equiv \frac{\Gamma_{inv}}{\Gamma_{\ell\bar{\ell}}} = N_\nu \left( \frac{\Gamma_{\nu\bar{\nu}}}{\Gamma_{\ell\bar{\ell}}} \right)_{SM}, \quad (5)$$

with  $N_\nu = 3$ . Here, the decay rate for the  $Z$  boson into charged leptons is given by [31]

$$\Gamma_{\ell\bar{\ell}} = \frac{G_F M_Z^3 (g_V^\ell{}^2 + g_A^\ell{}^2)}{6\sqrt{2}\pi} \quad (6)$$

where  $g_V^\ell$  and  $g_A^\ell$  are the vector and axial coupling for a charged lepton  $\ell$ :

$$g_V^\ell = T_\ell - 2Q_\ell \sin^2 \theta_W,$$

$$g_A^\ell = T_\ell.$$

When we consider the non-unitarity formalism, applied to the invisible decay rate of the  $Z$  boson, we will find that the contribution of the three active neutrino flavors will be given by [31]

$$\Gamma_{inv} = \frac{G_F M_Z^3 \sum_{i,j} |(N^\dagger N)_{ij}|^2}{12\sqrt{2}\pi}. \quad (7)$$

that can also be expressed as

$$\Gamma_{inv} = \frac{G_F M_Z^3 \sum_{\alpha,\beta} |(NN^\dagger)_{\alpha\beta}|^2}{12\sqrt{2}\pi}. \quad (8)$$

Comparing this expression with the unitary case discussed before, we can define for the non-unitary case

$$N_\nu = \sum_{\alpha,\beta} |(NN^\dagger)_{\alpha\beta}|^2. \quad (9)$$

It is important to notice that the theoretical expression for the decay rate will be affected by non-unitarity with several corrections. However, we must notice that there is another correction due to the definition of  $G_F$ . In order to introduce this correction, we can write the equivalent expression to Eq. (5) for the non-unitary case. For this purpose, we start by considering that, from muon decay, a non-unitary mixing will affect the value of the Fermi constant to be [7, 26, 32]

$$G_F = \frac{G_\mu}{\sqrt{\sum_{ij} |N_{\mu i}|^2 |N_{e j}|^2}} = \frac{G_\mu}{\sqrt{\alpha_{11}^2 (\alpha_{22}^2 + |\alpha_{21}|^2)}}. \quad (10)$$

This correction cancel out in the ratio,  $R_{inv}^0$ , but can propagate to other observables, such as the weak mixing angle [27]

$$\sin^2 \theta_W = \frac{1}{2} \left( 1 - \sqrt{1 - \frac{2\sqrt{2}\alpha\pi}{G_\mu M_Z^2} \sqrt{\alpha_{11}^2 (\alpha_{22}^2 + |\alpha_{21}|^2)}} \right). \quad (11)$$

From Eqs. (9) and (6), we can get an expression for the ratio in the non-unitary case:

$$R_{inv}^0 = \frac{\sum_{\alpha,\beta} |(NN^\dagger)_{\alpha\beta}|^2}{2(g_V^\ell{}^2 + g_A^\ell{}^2)}. \quad (12)$$

Let us notice that the deviation from unitarity, introduced by the parameters  $\alpha_{ij}$ , appears explicitly in the numerator through  $|(NN^\dagger)_{\alpha\beta}|^2$ , but also implicitly in the denominator via  $g_V^\ell$ , because it contains the expression for the weak mixing given in Eq. (11). The explicit

form for the numerator in the previous formula will be

$$\begin{aligned}
\sum_{\alpha,\beta} |(NN^\dagger)_{\alpha\beta}|^2 &= \alpha_{11}^4 + \alpha_{22}^4 + \alpha_{33}^4 + |\alpha_{21}|^4 + |\alpha_{31}|^4 + |\alpha_{32}|^4 \\
&+ 2\alpha_{22}^2|\alpha_{21}|^2 + 2\alpha_{33}^2(|\alpha_{31}|^2 + |\alpha_{32}|^2) + 2|\alpha_{31}|^2|\alpha_{32}|^2. \\
&+ 2\alpha_{11}^2(|\alpha_{21}|^2 + |\alpha_{31}|^2) + 2|\alpha_{21}\alpha_{31}^* + \alpha_{22}\alpha_{32}^*|^2
\end{aligned} \tag{13}$$

If we neglect terms including third order or higher on off-diagonal parameters ( $\alpha_{ij}$   $i \neq j$ ), we obtain the following reduced expression:

$$\sum_{\alpha,\beta} |(NN^\dagger)_{\alpha\beta}|^2 = \alpha_{11}^4 + \alpha_{22}^4 + \alpha_{33}^4 + 2\alpha_{11}^2(|\alpha_{21}|^2 + |\alpha_{31}|^2) + 2\alpha_{22}^2(|\alpha_{21}|^2 + |\alpha_{32}|^2) + 2\alpha_{33}^2(|\alpha_{31}|^2 + |\alpha_{32}|^2).$$

Different constraints for the  $\alpha_{ij}$  parameters show that  $N^{NP}$  is close to an identity matrix.

Besides, the precision of the measurements under consideration makes necessary to introduce radiative corrections. In the  $\overline{MS}$  scheme, the weak mixing angle takes the form [31]

$$\hat{s}_Z = \frac{A_0}{M_W(1 - \Delta\hat{r}_W)^{1/2}}, \tag{14}$$

where, in the non-unitary case,  $A_0$  is given by

$$A_0 = \left( \frac{\pi\alpha}{\sqrt{2}G_F} \right)^{1/2} = \left( \frac{\pi\alpha\sqrt{\alpha_{11}^2(\alpha_{22}^2 + |\alpha_{21}|^2)}}{\sqrt{2}G_\mu} \right)^{1/2}, \tag{15}$$

$\Delta\hat{r}_W$  introduces the radiative corrections, and  $M_W$  is the mass of the  $W$  boson. According to PDG [31], the values of the relevant parameters are:

$$M_W = 80.379 \pm 0.012 \text{ GeV}/c^2, \tag{16}$$

$$\Delta\hat{r}_W = 0.06916 \pm 0.00008, \tag{17}$$

$$\alpha = (7.2973525664 \pm 0.0000000017) \times 10^{-3}, \tag{18}$$

$$G_\mu = (1.1663787 \pm 0.0000006) \times 10^{-5} \text{ GeV}^2 \tag{19}$$

$$\hat{s}_Z^2 = 0.23122 \pm 0.00003. \tag{20}$$

For measurements at energies around the  $Z$  peak it is common to use the effective weak

mixing angle  $\bar{s}_t^2$  instead of the  $\overline{MS}$  scheme; both quantities are related through [31]  $\bar{s}_t^2 = \hat{s}_Z^2 + 0.00032$ .

Now we can turn now our attention to the comparison with the experimental results to obtain constraints and future perspectives for the NU parameters. However, before entering into this discussion we will also discuss another neutrino counting observable.

### B. The process $e^-e^+ \rightarrow \nu\bar{\nu}\gamma$

Another process that was also measured at LEP, and allows for a neutrino counting, is the single photon production with a neutrino-antineutrino pair [17, 33–42]. In this subsection we compute the expression for this observable in the NU case.

The differential cross section for the single photon production from electron-positron annihilation,  $e^+e^- \rightarrow \nu\bar{\nu}\gamma$ , can be written in terms of the radiator function  $H(x, y; s)$  and the “reduced” cross section for the process  $e^+e^- \rightarrow \nu\bar{\nu}$ ,  $\sigma_0$ , as [43, 44]:

$$\frac{d^2\sigma}{dx dy} = H(x, y; s) \sigma_0(s(1-x)). \quad (21)$$

The radiator function is defined by

$$H(x, y; s) = \frac{2\alpha}{\pi} \frac{[(1 - \frac{1}{2}x)^2 + \frac{1}{4}x^2y^2]}{x(1-y^2)}, \quad (22)$$

with

$$x = 2E_\gamma/\sqrt{s}, \quad y = \cos\theta_\gamma, \quad (23)$$

and  $\sigma_0$ , the “reduced” cross section for the process  $e^+e^- \rightarrow \nu\bar{\nu}$  is given by

$$\begin{aligned} \sigma_0(s) &= \sigma_W(s) + \sigma_Z(s) + \sigma_{W-Z}(s), \\ \sigma_0(s) &= \frac{G_F^2 s}{12\pi} \left[ 2 + \frac{N_\nu(g_V^2 + g_A^2)}{(1 - s/M_Z^2)^2 + \Gamma_Z^2/M_Z^2} + \frac{2(g_V + g_A)(1 - s/M_Z^2)}{(1 - s/M_Z^2)^2 + \Gamma_Z^2/M_Z^2} \right]. \end{aligned} \quad (24)$$

The three terms in Eq. (24) come from the contribution of the  $W$ , the  $Z$  boson, and their interference, as can be seen in the Feynman diagrams in Fig. 1.

For energies above de  $Z$  resonance, finite distance effects on the  $W$  propagator need to

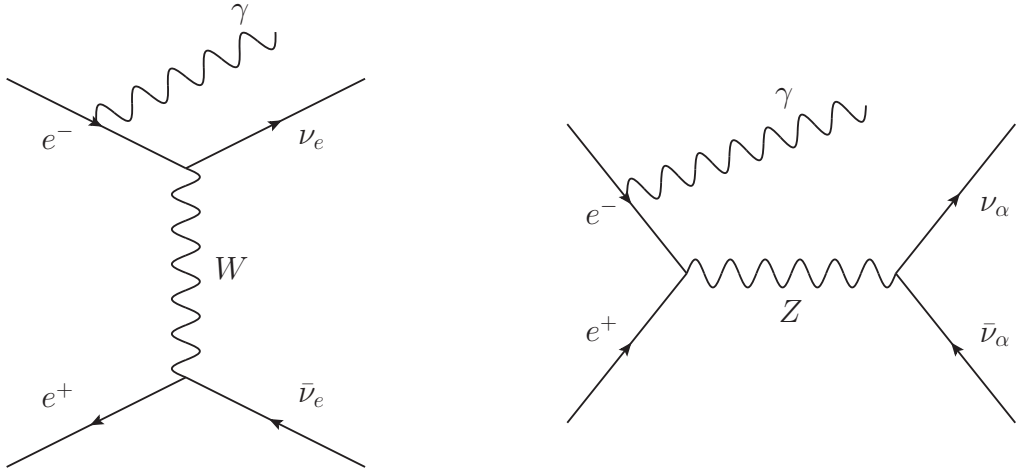


Figure 1: Contributions to the  $e^-e^+ \rightarrow \nu\bar{\nu}\gamma$  process.

be considered. These effects are taken into account by the following substitution [42, 44]:

$$\begin{aligned}\sigma_W(s) &\rightarrow \sigma_W(s)F_W(s/M_W^2) \\ \sigma_{W-Z}(s) &\rightarrow \sigma_{W-Z}(s)F_{W-Z}(s/M_W^2),\end{aligned}\tag{25}$$

where

$$\begin{aligned}F_W(z) &= \frac{3}{z^3} [-2(z+1)\log(z+1) + z(z+2)], \\ F_{W-Z}(z) &= \frac{3}{z^3} [(z+1)^2\log(z+1) - z(\frac{3}{2}z+1)].\end{aligned}\tag{26}$$

From Eq. (21), the total cross section is

$$\sigma(s) = \int_{x_{\min}}^1 dx \int_{-\cos\theta_{\min}}^{\cos\theta_{\min}} dy H(x, y; s) \sigma_0(s(1-x)).\tag{27}$$

If we now examine this process in a nonunitary mixing framework, it is almost straight-

forward to obtain the nonunitary effects in the reduced cross section:

$$\begin{aligned}
\sigma_0^{NU}(s) &= \sum_{i,j} |N_{ei}|^2 |N_{ej}|^2 \sigma_W(s) F_W(s/M_W^2) \\
&+ \sum_{\alpha,\beta} |(NN^\dagger)_{\alpha\beta}|^2 \sigma_Z(s) \\
&+ \sum_{i,j} |N_{ei}|^2 |N_{ej}|^2 \sigma_{W-Z}(s) F_{W-Z}(s/M_W^2).
\end{aligned} \tag{28}$$

These corrections can be seen in Fig. 1: for the  $W$  contribution (left diagram), each neutrino line contributes with a term  $U_{ei}$  in the scattering amplitude, while for the  $Z$  contribution (right diagram), the provided correction is of the form  $U_{\alpha i}$ . Since the mixing is nonunitary, flavor-changing neutral currents are allowed, hence the sum must be given over different flavors in the second term of Eq. (28).

Writing Eq. (28) explicitly, we will have

$$\begin{aligned}
\sigma_0^{NU}(s) &= \frac{G_F^2 s}{12\pi} \left[ 2 \sum_{i,j} |N_{ei}|^2 |N_{ej}|^2 \right. \\
&+ \sum_{\alpha,\beta} |(NN^\dagger)_{\alpha\beta}|^2 \frac{(g_V^2 + g_A^2)}{(1 - s/M_Z^2)^2 + \Gamma_Z^2/M_Z^2} \\
&\left. + \sum_{i,j} |N_{ei}|^2 |N_{ej}|^2 \frac{2(g_V + g_A)(1 - s/M_Z^2)}{(1 - s/M_Z^2)^2 + \Gamma_Z^2/M_Z^2} \right].
\end{aligned} \tag{29}$$

Additionally, as discussed in the previous subsection, there will be NU corrections to  $G_F$  and  $\sin^2 \theta_W$  as described in Eqs. (10) and (11), respectively. Finally, it should be noticed that in the last two terms of Eq. (28), the decay width,  $\Gamma_Z$ , appears in the denominator. Since we are considering the NU case, we must also introduce the corresponding corrections. The total  $Z$  decay width can be calculated as [30, 31]

$$\Gamma_Z = \Gamma_{\text{inv}} + \Gamma_{\ell\ell} + \Gamma_{\text{had}} \tag{30}$$

and the nonunitary correction will appear through the  $\Gamma_{\text{inv}}$  contribution, as it had been

computed in the previous subsection, and we will have:

$$\Gamma_Z = \frac{G_F M_Z^3}{12\sqrt{2}\pi} \sum_{\alpha,\beta} |(NN^\dagger)_{\alpha\beta}|^2 + \Gamma_{\ell\ell} + \Gamma_{\text{had}}. \quad (31)$$

Now that we have introduced the theoretical expressions for the two neutrino counting observables with the formalism for the non-unitary case, in the triangular parametrization, we will discuss the corresponding current constraints and future perspectives for these two cases.

### III. EXPERIMENTAL TESTS

#### A. The process $e^-e^+ \rightarrow \nu\bar{\nu}\gamma$

To obtain constraints for the NU case from the process  $e^-e^+ \rightarrow \nu\bar{\nu}\gamma$ , we use the reported measurements from the ALEPH collaboration [17]. They are listed in Table I. The center of mass energy for each run is listed in the first column. The background subtracted measured and Monte Carlo cross sections are given in columns two and three, respectively. The number of observed events after background subtraction are given in column four, while the efficiency corresponds to column five. Lastly, the kinematical cuts for the outgoing photon energy and angle are reported in the last two columns. For these cuts,  $x_T = x \sin \theta_\gamma$  (with  $x = E_\gamma/E_{\text{beam}}$ ), while  $y = \cos \theta_\gamma$ .

$\sqrt{s}$ (GeV)	$\sigma^{\text{mes}}$ (pb)	$\sigma^{\text{MC}}$ (pb)	$N_{\text{obs}}$	$\epsilon(\%)$	$E_\gamma$ (GeV)	$ y $
189	$3.43 \pm 0.17$	$3.48 \pm 0.05$	484			
192	$3.47 \pm 0.40$	$3.23 \pm 0.05$	81			
196	$3.03 \pm 0.23$	$3.26 \pm 0.05$	197			
200	$3.23 \pm 0.22$	$3.12 \pm 0.05$	231	81.5	$x_T \geq 0.075$	$\leq 0.95$
202	$2.99 \pm 0.29$	$3.07 \pm 0.05$	110			
205	$2.84 \pm 0.22$	$2.93 \pm 0.05$	182			
207	$2.67 \pm 0.17$	$2.80 \pm 0.05$	292			

Table I: Summary from the ALEPH collaboration experimental data, collected above the  $W^+W^-$  production threshold [17].

In order to make our analysis, we have computed the cross section from Eqs. (27) and (29), with the integration limits taken according to the last two columns of Table I. We have

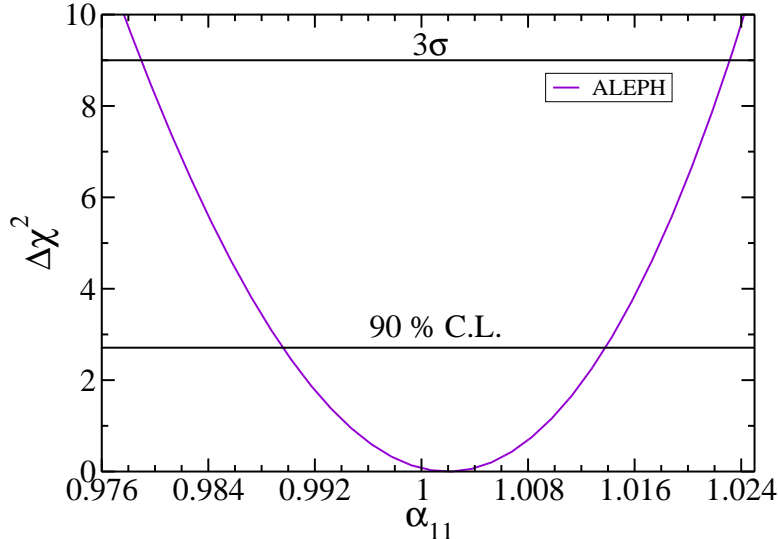


Figure 2: Bounds on the NU parameter  $\alpha_{11}$  from the process  $e^-e^+ \rightarrow \nu\bar{\nu}\gamma$ , using the ALEPH reported results.

checked that our integration in the unitary limit is in fare agreement with the reported Monte Carlo simulation for each center of mass energy measurement.

Once we have obtained this expression, we have compared our theoretical expectation for the NU case with the experimental results of Table I through a  $\chi^2$  analysis.

Our result for the non-unitary parameter  $\alpha_{11}$  is shown in Fig. 2. In this analysis, we have considered any other NU parameter as equal to the Standard case, that is,  $\alpha_{22}^2 = \alpha_{33}^2 = 1$  and  $\alpha_{21}^2 = \alpha_{31}^2 = \alpha_{32}^2 = 0$ . We have choosen this parameter because diagonal parameters  $\alpha_{ii}$  give the main contribution for deviations from unitarity. Besides, any diagonal parameter contributes on equal footing and, therefore, our constrain can be equally applied to  $\alpha_{22}$  or  $\alpha_{33}$ . As it can be seen, it is possible to restrict the  $\alpha_{11}$  NU parameter, and the constraint at 90 % CL is given by

$$\alpha_{11} > 0.9896, \quad 1 - \alpha_{11} < 0.0104. \quad (32)$$

To our knowledge, this is the first time that a constraint for NU is reported using this observable and it is possible to see that the limits are competitive. A more detailed analysis, using for example data from DELPHI [35], L3 [36–38] and OPAL [39–41], could give more restrictive results, although the details of the cuts for these cases could make the analysis more challenging.

## B. The invisible Z decay

We now turn our attention to the particular case of the  $Z$  decay into neutrinos. This process has already been measured by LEP [15, 16] and future experiments [1–4, 19–24] can improve the measurement of this important observable. Previous works have already reported constraints on NU parameters using this observable for a combined analysis from different measurements [27, 45–47]. Here we focus in this particular parameter using the specific triangular parametrization and making more emphasis in the perspectives from future experimental proposals.

Before analyzing the invisible decay constraints on NU, it is important to remember from the previous section that the NU case will affect the theoretical prediction of different parameters, such as  $G_F$  and  $\sin^2 \theta_W$  (Eqs. (10) and (11), respectively.) Perhaps the most important observable for our discussion is the value of the weak mixing angle that, at the relevant energy, differs up to three standard deviations depending on the experiment that measures it. Its impact is illustrated in Fig. 3, where we show the  $\chi^2$  curve for this observable as a function of the  $\alpha_{11}$  parameter. In this figure, besides considering the LEP [15, 16] measurement for the weak mixing angle, we also show how this constraint changes if we consider other measurements for the weak mixing angle. That is the case of the Tevatron [48–51], Atlas [52], LHCb [53] and CMS [54] result. It is possible to notice that the evaluation of this fundamental quantity of the Standard Model still can have an impact on the non-unitarity constraints. As in the previous subsection, for this plot we have only considered  $\alpha_{11}$  as different from one and all other non-unitary parameters as equal to the standard case, that is,  $\alpha_{22}^2 = \alpha_{33}^2 = 1$  and  $\alpha_{21}^2 = \alpha_{31}^2 = \alpha_{32}^2 = 0$ .

Provided that we have a precise measurement of the weak mixing angle, we can return to the computation of constraints on NU from current and future experimental proposals that will improve the measurements of different observables, such as the number of neutrinos,  $N_\nu$ , or the effective value of the weak mixing angle,  $\sin^2 \theta_{eff}$ . We show their sensitivity in Table II.

In order to estimate the sensitivity of the future experiments we will consider again the ratio given by Eq. (5). In particular, the uncertainty of  $R_{inv}^0$  is calculated from

$$\sigma^2(R_{inv}^0) = \left( \frac{\Gamma_{\nu\bar{\nu}}}{\Gamma_{\bar{u}u}} \right)_{SM}^2 \sigma^2(N_\nu) + (N_\nu)^2 \sigma^2 \left( \frac{\Gamma_{\nu\bar{\nu}}}{\Gamma_{\bar{u}u}} \right)_{SM},$$

	LEP [15]	CEPC [4]	FCC-ee [2]	ILC [1]
$\sigma(N_\nu)$	0.008	0.003	0.004	0.004
$\sigma(\sin^2 \theta_{eff})$	0.00016	0.000023	—	0.00001

Table II: Expected uncertainties on  $N_\nu$  and  $\sin^2 \theta_{eff}$  for different experimental proposals. Notice that for LEP we quote the present experimental values, whereas for CEPC, FCC-ee, and ILC we show future estimations.

CEPC			
$R_{inv}^0$	$5.9430 \pm 0.0065$	$5.9671 \pm 0.0065$	$5.9801 \pm 0.0065$
FCC-ee / ILC			
$R_{inv}^0$	$5.9430 \pm 0.0065$	$5.9671 \pm 0.0065$	$5.9801 \pm 0.0065$

Table III: Test values for the invisible ratio  $R_{inv}^0$  used in the present work. We quote the expected uncertainty coming from future experiments.

where  $\sigma\left(\frac{\Gamma_{\nu\bar{\nu}}}{\Gamma_{ii}}\right)_{SM} = 0.00083$  [15] and  $\sigma(N_\nu)$  is given in Table II. With these hypothesis we obtain the results shown in Table III.

Within this framework, it is possible to obtain an idea of the future sensitivity of these experiments on the NU parameters. A forecast for this sensitivity can be computed considering three different cases of a future measurement of the ratio  $R_{inv}^0$ :

- The experimental value reported at [15],  $R_{inv}^0 = 5.9430$ .

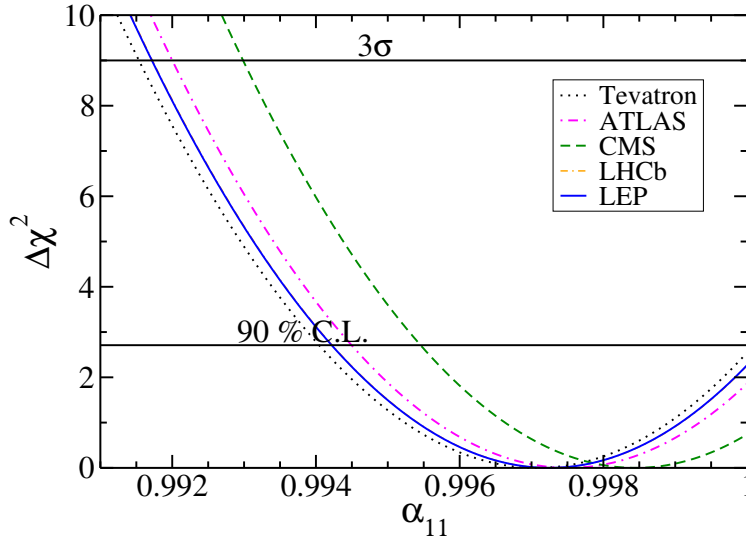


Figure 3: Restrictions for  $\alpha_{11}$  from the invisible decay of the  $Z$  boson, depending on the value of the effective weak mixing angle,  $\bar{s}_l^2$ . We consider the measurements on  $\bar{s}_l^2$  coming from different experiments.

Experiment	$R_{inv}^0$	$\alpha_{11}$	$\alpha_{11}$ ( $\alpha_{31}$ and $\alpha_{33}$ free)
current	5.9430	$0.99403 < \alpha_{11}$	$0.99403 < \alpha_{11}$
CEPC	5.9430	$0.99602 < \alpha_{11} < 0.99847$	$0.99602 < \alpha_{11}$
FCC-ee/ILC	5.9430	$0.99568 < \alpha_{11} < 0.99881$	$0.99568 < \alpha_{11}$
CEPC	5.9671	$0.99879 < \alpha_{11} < 1.00123$	$0.99879 < \alpha_{11} < 1.00123$
FCC-ee/ILC	5.9671	$0.99844 < \alpha_{11} < 1.00156$	$0.99845 < \alpha_{11} < 1.00157$
CEPC	5.9801	$1.00026 < \alpha_{11} < 1.00269$	$1.00027 < \alpha_{11} < 1.00270$
FCC-ee/ILC	5.9801	$0.99993 < \alpha_{11}; < 1.00305$	$0.99994 < \alpha_{11} < 1.00304$

Table IV: Allowed values for  $\alpha_{11}$  at 90% C.L., considering present experimental values and future proposals from CEPC, FCC-ee and ILC experiments. We consider either the case when any NU parameter other than  $\alpha_{11}$  is in the unitary limit and also when  $\alpha_{31}$  and  $\alpha_{33}$  are allowed to vary, fulfilling the Cauchy-Schwartz condition.

- The theoretical value calculated from the effective weak mixing angle including radiative corrections [55],  $R_{inv}^0 = 5.9671$ .
- A value two standard deviations (of CEPC) above of the previous value,  $R_{inv}^0 = 5.9801$ .

For these three cases, we perform a  $\chi^2$  analysis in order to have a forecast of the future expected sensitivity, considering the following two scenarios:

- First, we consider that  $\alpha_{11}$  is the only parameter different from the standard case. The  $\chi^2$  fit is made with the errors already discussed for each experiment. The results are compiled in Fig. 4.
- Second, we let  $\alpha_{11}$ ,  $\alpha_{13}$  and  $\alpha_{33}$  to vary freely, while fulfilling the Cauchy-Schwarz condition:

$$|\alpha_{ij}| \leq \sqrt{(1 - \alpha_{ii}^2)(1 - \alpha_{jj}^2)}. \quad (33)$$

The other NU parameters are set to their SM value. The results obtained are shown in Fig.5. Notice that we have considered only  $\alpha_{33}$  and  $\alpha_{31}$  different from zero, since very similar results will be obtained with  $\alpha_{22}$  and  $\alpha_{21}$ .

We summarize the expected accuracy for both cases in Table IV. We can see from these results that future collider experiments could give a constraint on the diagonal non-unitary parameter that will be stronger than the current global limits [11, 13], that constraints  $\alpha_{11}$  at the level of 0.999 or below.

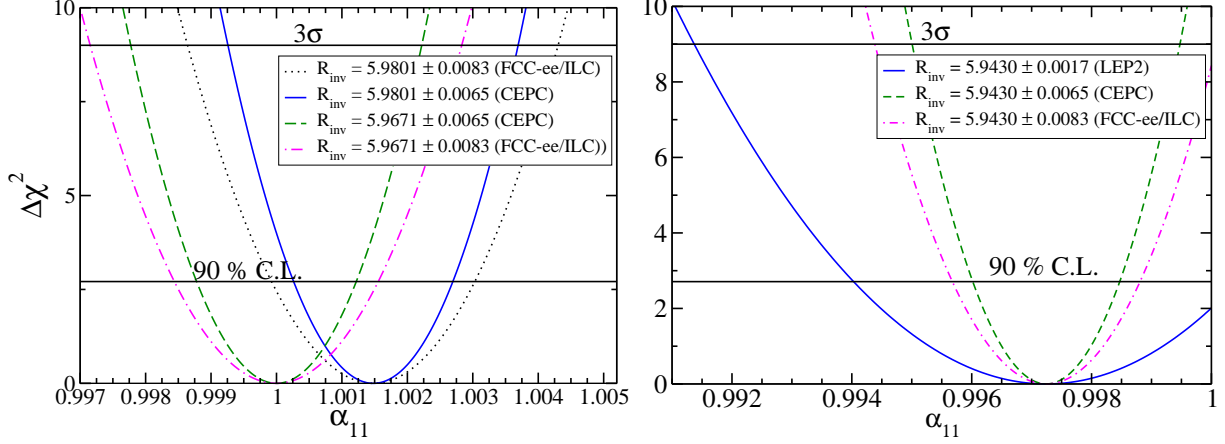


Figure 4: Restrictions for  $\alpha_{11}$  from the invisible decay of the  $Z$  boson, for the future proposals CEPC, FCC-ee and ILC experiments. We have considered different possible central values to illustrate the constraints to be obtained.

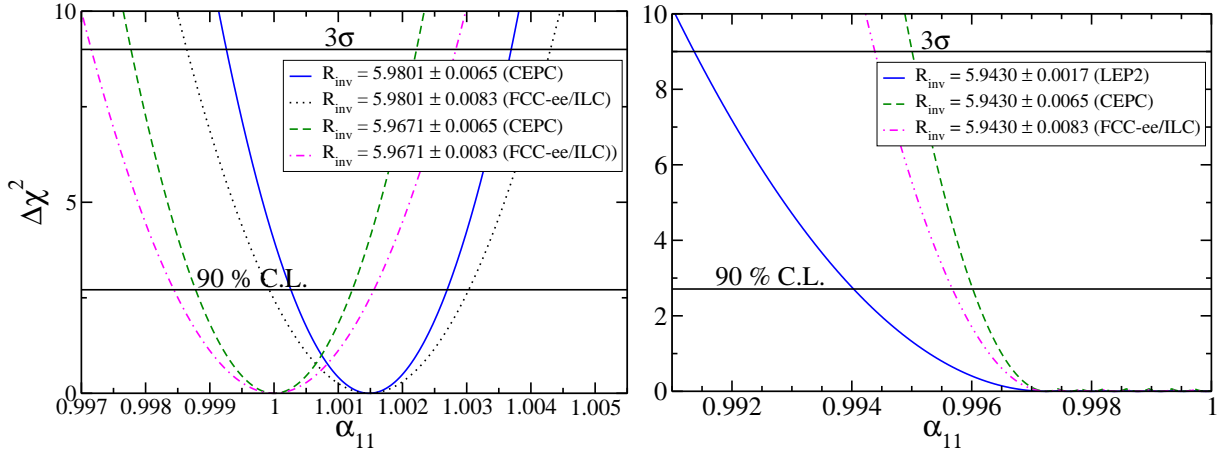


Figure 5: Restrictions for  $\alpha_{11}$  from the invisible decay of the  $Z$  boson for the future CEPC, FCC-ee and ILC experiments. Different central values have been used as a test to illustrate the possible constraints. For this case, we have considered  $\alpha_{33}$  and  $\alpha_{31}$  as free parameters in the fit (fulfilling the Cauchy-Schwartz condition).

#### IV. CONCLUSIONS

We have reviewed the measurements for neutrino counting observables close to the  $Z$  peak and reported a new analysis for the non-unitary formalism for the case of the  $\nu\bar{\nu}\gamma$  process. The corresponding constraints have been introduced in this work and we have shown that they are competitive with other current constraints. As far as we know, this is the first time this analysis is done. We have used the triangular parametrization to perform this analysis.

We have also analyzed the invisible  $Z$  decay into neutrinos, in the same triangular parametrization. In this case we have focused in the importance of a precise determination of the weak mixing angle and in the perspectives to improve current constraints by using future collider experiments, that are expected to be constructed as a continuation of the precision program for particle physics. They will allow to obtain better restrictions to new physics from several processes at different energy regimes. For this purpose, we have focused in the invisible decay width in the  $Z$  peak, that will be measured in the first stages of the future collider experiments ILC, FCC-ee and CEPC.

We have shown that any of these experiments will have enough sensitivity to improve the current constraint on non-unitarity, we have focused especially in the diagonal parameter  $\alpha_{11}$ . To obtain this result we have used different test values. In particular, for a measurement as low as the current LEP central value, future experiments will give a positive signal for non-unitarity at 90 % C. L. while a future measurement in accordance with the Standard model prediction will restrict the limit for  $\alpha_{11}$  to be bigger than 0.999, that is, a precision at the level of  $10^{-3}$ . It is also important to notice that, as can be seen from Eq. (13), the  $Z$  decay measurement will mainly restrict the sum of the three diagonal parameters:  $\sum_i \alpha_{ii}$  and, therefore, in a combined analysis, this measurement will help to restrict any of the diagonal parameters.

## V. ACKNOWLEDGMENTS

This work was supported by the Conacyt grant A1-S-23238 and SNI (Mexico). LJF also thanks the Conacyt for the grant of Ayudante de investigador (EXP. AYTE. 16959).

- 
- [1] H. Baer, T. Barklow, K. Fujii, Y. Gao, A. Hoang, S. Kanemura, J. List, H. E. Logan, A. Nomerotski, M. Perelstein, et al. (2013), 1306.6352.
  - [2] M. Bicer et al. (TLEP Design Study Working Group), JHEP **01**, 164 (2014), 1308.6176.
  - [3] M. Dong et al. (CEPC Study Group) (2018), 1811.10545.
  - [4] M. Ahmad et al. (TLEP Design Study Working Group) (2015).
  - [5] M. J. Boland et al. (CLICdp, CLIC) (2016), 1608.07537.
  - [6] J. Schechter and J. W. F. Valle, Phys. Rev. **D22**, 2227 (1980).

- [7] E. Nardi, E. Roulet, and D. Tommasini, Phys. Lett. **B327**, 319 (1994), hep-ph/9402224.
- [8] A. de Gouvêa and A. Kobach, Phys. Rev. **D93**, 033005 (2016), 1511.00683.
- [9] A. Yu. Smirnov and R. Zukanovich Funchal, Phys. Rev. **D74**, 013001 (2006), hep-ph/0603009.
- [10] F. J. Escrihuela, D. V. Forero, O. G. Miranda, M. Tortola, and J. W. F. Valle, Phys. Rev. **D92**, 053009 (2015), [Erratum: Phys. Rev.D93,no.11,119905(2016)], 1503.08879.
- [11] F. J. Escrihuela, D. V. Forero, O. G. Miranda, M. Tórtola, and J. W. F. Valle, New J. Phys. **19**, 093005 (2017), 1612.07377.
- [12] O. G. Miranda and J. W. F. Valle, Nucl. Phys. **B908**, 436 (2016), 1602.00864.
- [13] M. Blennow, P. Coloma, E. Fernandez-Martinez, J. Hernandez-Garcia, and J. Lopez-Pavon, JHEP **04**, 153 (2017), 1609.08637.
- [14] M. C. Gonzalez-Garcia, A. Santamaria, and J. W. F. Valle, Nucl. Phys. **B342**, 108 (1990).
- [15] S. Schael et al. (SLD Electroweak Group, DELPHI, ALEPH, SLD, SLD Heavy Flavour Group, OPAL, LEP Electroweak Working Group, L3), Phys. Rept. **427**, 257 (2006), hep-ex/0509008.
- [16] S. Schael et al. (DELPHI, OPAL, LEP Electroweak, ALEPH, L3), Phys. Rept. **532**, 119 (2013), 1302.3415.
- [17] A. Heister et al. (ALEPH), Eur. Phys. J. **C28**, 1 (2003).
- [18] M. Carena, A. de Gouvea, A. Freitas, and M. Schmitt, Phys. Rev. **D68**, 113007 (2003), hep-ph/0308053.
- [19] J. Fan, M. Reece, and L.-T. Wang, JHEP **09**, 196 (2015), 1411.1054.
- [20] M. Baak et al., in *Proceedings, 2013 Community Summer Study on the Future of U.S. Particle Physics: Snowmass on the Mississippi (CSS2013): Minneapolis, MN, USA, July 29-August 6, 2013* (2013), 1310.6708, URL <http://www.slac.stanford.edu/econf/C1307292/docs/EnergyFrontier/Electroweak-19.pdf>.
- [21] S. Banerjee, P. S. B. Dev, A. Ibarra, T. Mandal, and M. Mitra, Phys. Rev. **D92**, 075002 (2015), 1503.05491.
- [22] A. Blondel, E. Graverini, N. Serra, and M. Shaposhnikov (FCC-ee study Team), Nucl. Part. Phys. Proc. **273-275**, 1883 (2016), 1411.5230.
- [23] W. Liao and X.-H. Wu, Phys. Rev. **D97**, 055005 (2018), 1710.09266.
- [24] H. Liang and M. Ruan, Int. J. Mod. Phys. Conf. Ser. **46**, 1860086 (2018).
- [25] M. Gronau, C. N. Leung, and J. L. Rosner, Phys. Rev. **D29**, 2539 (1984).
- [26] A. Atre, T. Han, S. Pascoli, and B. Zhang, JHEP **05**, 030 (2009), 0901.3589.

- [27] E. Fernandez-Martinez, J. Hernandez-Garcia, and J. Lopez-Pavon, *JHEP* **08**, 033 (2016), 1605.08774.
- [28] H. Hettmansperger, M. Lindner, and W. Rodejohann, *JHEP* **04**, 123 (2011), 1102.3432.
- [29] W. Rodejohann and J. W. F. Valle, *Phys. Rev.* **D84**, 073011 (2011), 1108.3484.
- [30] E. K. Akhmedov, in *Proceedings, Summer School in Particle Physics: Trieste, Italy, June 21-July 9, 1999* (1999), pp. 103–164, hep-ph/0001264.
- [31] M. Tanabashi et al. (Particle Data Group), *Phys. Rev.* **D98**, 030001 (2018).
- [32] P. Langacker and D. London, *Phys. Rev.* **D38**, 886 (1988).
- [33] R. Barate et al. (ALEPH), *Phys. Lett.* **B420**, 127 (1998), hep-ex/9710009.
- [34] R. Barate et al. (ALEPH), *Phys. Lett.* **B429**, 201 (1998).
- [35] P. Abreu et al. (DELPHI), *Eur. Phys. J.* **C17**, 53 (2000), hep-ex/0103044.
- [36] M. Acciarri et al. (L3), *Phys. Lett.* **B415**, 299 (1997).
- [37] M. Acciarri et al. (L3), *Phys. Lett.* **B444**, 503 (1998).
- [38] M. Acciarri et al. (L3), *Phys. Lett.* **B470**, 268 (1999), hep-ex/9910009.
- [39] K. Ackerstaff et al. (OPAL), *Eur. Phys. J.* **C2**, 607 (1998), hep-ex/9801024.
- [40] G. Abbiendi et al. (OPAL), *Eur. Phys. J.* **C8**, 23 (1999), hep-ex/9810021.
- [41] G. Abbiendi et al. (OPAL), *Eur. Phys. J.* **C18**, 253 (2000), hep-ex/0005002.
- [42] M. Hirsch, E. Nardi, and D. Restrepo, *Phys. Rev.* **D67**, 033005 (2003), hep-ph/0210137.
- [43] O. Nicosini and L. Trentadue, *Nucl. Phys.* **B318**, 1 (1989).
- [44] J. Barranco, O. G. Miranda, C. A. Moura, and J. W. F. Valle, *Phys. Rev.* **D77**, 093014 (2008), 0711.0698.
- [45] S. Antusch and O. Fischer, *JHEP* **10**, 094 (2014), 1407.6607.
- [46] S. Antusch and O. Fischer, *JHEP* **05**, 053 (2015), 1502.05915.
- [47] O. Fischer and S. Antusch, *PoS DIS2017*, 090 (2018), 1709.00880.
- [48] V. M. Abazov et al. (D0), *Phys. Rev.* **D84**, 012007 (2011), 1104.4590.
- [49] D. Acosta et al. (CDF), *Phys. Rev.* **D71**, 052002 (2005), hep-ex/0411059.
- [50] T. A. Aaltonen et al. (CDF, D0), *Phys. Rev.* **D88**, 052018 (2013), 1307.7627.
- [51] (2010), 1003.2826.
- [52] G. Aad et al. (ATLAS), *JHEP* **09**, 049 (2015), 1503.03709.
- [53] R. Aaij et al. (LHCb), *JHEP* **11**, 190 (2015), 1509.07645.
- [54] S. Chatrchyan et al. (CMS), *Phys. Rev.* **D84**, 112002 (2011), 1110.2682.

[55] C. Patrignani et al. (Particle Data Group), *Chin. Phys.* **C40**, 100001 (2016).